



Cite this: *Environ. Sci.: Processes Impacts*, 2026, **28**, 112

## Feasibility of microbial-induced calcite precipitation in soils polluted by hydrocarbons

Carla Comadran-Casas, <sup>\*,a</sup> Philip J. Salter, <sup>b</sup> Ayo Ogundero, <sup>a</sup> Fabien Cholet, <sup>a</sup> Victor Barridor Giadom, <sup>a</sup> William T. Sloan, <sup>a</sup> Cindy J. Smith, <sup>a</sup> Adrian M. Bass, <sup>c</sup> John MacDonald, <sup>c</sup> Cise Unluer <sup>d</sup> and Caroline Gauchotte-Lindsay <sup>\*,a</sup>

Microbial-Induced Calcite Precipitation (MICP) is an effective bioremediation method for heavy metals, which often co-exist with organic pollutants in soils. Organic pollutants such as hydrocarbons inhibit soil urea hydrolysis critical in MICP whilst its feasibility in such environments is poorly understood. This study presents an investigation on the potential of biostimulation and bioaugmentation of MICP in soils polluted by polycyclic aromatic hydrocarbons (PAH) and their effect on ureolysis at cell and enzyme level. Biostimulation of urea hydrolysis by soil autochthonous ureolytic bacteria was not detected over 62 days. Flow cytometry revealed *Sproposarcina pasteurii* at initial  $OD_{600} = 0.01$  was able to grow in soil water extracts of increasing hydrocarbon concentration ( $TOC = 0.035\text{--}35\text{ mg L}^{-1}$ ), showing no negative effects on cell membrane stability. Urease activity assays in soil water extracts inoculated with *S. pasteurii* ( $OD_{600} = 0.01$  and 1) and soybean *Glycine Max* urease enzyme (1 and  $100\text{ g L}^{-1}$ ) indicated hydrocarbons negative effect on cell and enzyme urease activity was dependant on hydrocarbon and cell/enzyme concentrations, indicating the mechanism of inhibition was competitive. *Glycine Max* urease activity was unaffected at  $100\text{ g L}^{-1}$  but at  $1\text{ g L}^{-1}$  decreased with increasing hydrocarbon concentration up to 61%, whilst *S. pasteurii* urease activity ( $OD_{600} = 1$ ) readily decreased at the lowest hydrocarbon concentration ( $TOC = 0.35\text{ mg L}^{-1}$ ) to an overall reduction of 31% at the highest TOC concentration. Bioaugmentation of *S. pasteurii* ( $OD_{600} = 1$ ) inoculated in the soil matrix successfully hydrolysed urea within 24 h. These results evidence for the first time the ability of model MICP bacteria *S. pasteurii* to grow and maintain relevant metabolic ureolytic activity in soils significantly polluted by PAH.

Received 10th July 2025  
Accepted 9th November 2025

DOI: 10.1039/d5em00531k

rsc.li/espi

### Environmental significance

Microbial-Induced Calcite Precipitation (MICP) in soils polluted by organic contaminants is poorly understood. This research evidences for the first time the feasibility of MICP in soils heavily polluted by polycyclic aromatic hydrocarbons.

## Introduction

Soil contaminants including trace elements (e.g., Cd, Pb, Cu, Zn, As), radionuclides (e.g.,  $^{90}\text{Sr}$ ), organic pollutants (e.g., hexachlorocyclohexanes, polycyclic aromatic hydrocarbons, polychlorinated biphenyls, polybrominated diphenyl ethers) and emerging contaminants (e.g., pharmaceuticals, plastics, nanomaterials) are a global pressing issue with severe negative effects both on the environment and humans.<sup>1</sup> An effective bioremediation method for heavy metals is their

immobilisation *via* incorporation into calcium carbonate ( $\text{CaCO}_3$ ) minerals through Microbial-Induced Calcite Precipitation (MICP), where toxic elements (e.g.  $\text{Cr}^{6+}$ ,<sup>2-4</sup>  $\text{Pb}^{2+}$ ,<sup>5,6</sup>  $\text{Sr}^{2+}$ ,<sup>7</sup>  $\text{Cd}^{2+}$ ,<sup>8,9</sup>  $\text{Zn}^{2+}$ ,<sup>8,9</sup>  $\text{As}^{3+}$ ,<sup>10</sup>  $\text{Ni}^{2+}$ ,<sup>11</sup>  $\text{Cu}^{2+}$ ,<sup>12</sup>) substitute calcium ( $\text{Ca}^{2+}$ ) forming stable and insoluble phases.

An important unexplored avenue of MICP in the context of bioremediation is its feasibility in soils polluted by organic contaminants. High molecular weight persistent organic pollutants such as polycyclic aromatic hydrocarbons (PAH) accumulate on surficial soils near source points<sup>13</sup> resulting in higher concentrations in industrial and urban centres<sup>14</sup> where they co-exist with heavy metals.<sup>15</sup> At present, the lack of knowledge on the effect of PAH on MICP constitutes a critical gap of relevance for the effective remediation of heavy metals in soil environments co-polluted by hydrocarbons.

MICP is a biogeochemical process that requires abundance of carbonate ( $\text{CO}_3^{2-}$ ) and  $\text{Ca}^{2+}$  ions and an alkaline pH (>8.5).

<sup>a</sup>James Watt School of Engineering, The University of Glasgow, UK. E-mail: Carla.ComadranCasas@glasgow.ac.uk

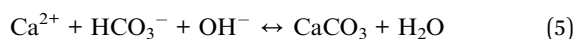
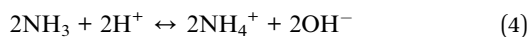
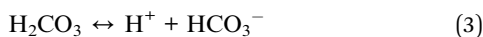
<sup>b</sup>Department of Civil & Environmental Engineering University of Strathclyde, Glasgow, UK

<sup>c</sup>School of Geographical & Earth Sciences, University of Glasgow, Glasgow, UK

<sup>d</sup>Department of Civil Engineering and Management, University of Manchester, Manchester, UK



These conditions are achieved through multiple bacterial metabolic pathways (ammonification, denitrification, sulphate and iron reduction).<sup>16</sup> Among these, ammonification of urea, or ureolysis, is mostly studied due to ubiquitousness of bacteria<sup>17</sup> and robustness against environmental conditions.<sup>18–21</sup> Ureolytic bacteria catalyse the hydrolysis of urea into ammonia (NH<sub>3</sub>) and carbamic acid (NH<sub>2</sub>COOH) by means of the urease enzyme (eqn (1)). NH<sub>2</sub>COOH spontaneously hydrolyses into NH<sub>3</sub> and carbonic acid (H<sub>2</sub>CO<sub>3</sub>) (eqn (2)), which subsequently equilibrate with water as bicarbonate (HCO<sub>3</sub><sup>−</sup>) and ammonium (NH<sub>4</sub><sup>+</sup>) ions (eqn (3)) and ((4)). The excess of hydroxide ions (OH<sup>−</sup>) between pH 6.3 and 9.3 (pK<sub>1</sub> and pK<sub>a</sub>, respectively) results in a net increase in pH, shifting HCO<sub>3</sub><sup>−</sup> speciation to CO<sub>3</sub><sup>2−</sup>. Provided the presence of Ca<sup>2+</sup>, CaCO<sub>3</sub> precipitation ensues (eqn (5)).<sup>22</sup>



In soils polluted by organic contaminants, urease activity has been investigated as a biomarker to assess soil pollution. Petroleum hydrocarbons have been shown to stimulate<sup>23–27</sup> and impair<sup>27–31</sup> soil urea hydrolysis. This has been shown to be dependent on pollutant concentration,<sup>28,31</sup> type of hydrocarbon,<sup>26,32</sup> co-presence of inorganic pollutants (*e.g.*, heavy metals),<sup>30,33</sup> as well as soil properties (*e.g.*, total organic carbon, pH),<sup>27</sup> nutrient availability (*e.g.*, phosphorous),<sup>24</sup> and incubation time.<sup>26,30</sup> However, little is known about the effects of PAH on ureolytic bacteria at molecular scale. Inhibition of urea hydrolysis may occur at cell and/or enzyme level, yet the exact mechanisms remain unclear. At cell level, it has been postulated that lipophilic compounds such as PAH have a narcotic mode of toxic action on bacteria, interacting with lipophilic components of bacteria cytoplasmic membranes and affecting their permeability and structure.<sup>34,35</sup> Narcosis is produced by non-specific binding of pollutants to cell membranes, dissolving or disrupting their fluidity and function and hence is dependent on pollutant lipophilicity.<sup>36</sup> At enzyme level, organic compounds are thought to denature the entire protein structure<sup>30</sup> and cause loss of catalytic function through interaction with functional groups of the enzyme active site and residues critical to maintaining its conformation.<sup>37</sup>

Understanding the effect of persistent organic pollutants such as PAH on ureolytic bacteria and ureolysis is important for the development of MICP applications in bioremediation and biogeotechnics in environments of anthropogenic and ecological relevance due to their widespread presence and co-existence with other pollutants (*e.g.*, heavy metals). As a first step towards this goal, this study aimed to elucidate the feasibility of MICP in presence of PAH by investigating PAH effect on ureolytic bacteria growth and ureolysis. Firstly, we investigated the response of a soil

from a gas plant heavily polluted by PAH to the application of urea over two months to determine the feasibility of MICP biostimulation approaches. Secondly, we investigated the viability of model MICP bacterium *S. pasteurii* growth in PAH polluted soil extracts at varying concentrations to determine its potential to grow once introduced in the polluted environment. Thirdly, we conducted urease activity assays in PAH polluted soil water extracts at varying cell, urease enzyme and PAH concentrations, under the hypothesis of increasing urease activity inhibition with increasing hydrocarbon concentration. The inhibitory effect of PAH on urease activity was investigated on *S. pasteurii* and soybean (*Glycine Max*) extracted plant urease to elucidate inhibition mechanisms at cell and enzyme level. Ureases exhibit high homology of amino acid sequences across species, such that the active site is conserved and induces the same mechanism of catalytic activity,<sup>38</sup> making plant and bacterial urease activity assays adequate to investigate inhibition mechanisms at cell and enzyme level. Based on the obtained results, we induced MICP by bioaugmentation of *S. pasteurii* on the PAH polluted soil. The results of this study provide, for the first time, scientific evidence of the feasibility of MICP in soil environments polluted by PAH.

## Materials and methods

### Soil samples

A soil polluted by coal tar (COV14) was sourced from a gas plant (England, UK) in which the main contaminants are PAH as described in Gauchotte-Lindsay *et al.*<sup>39</sup> An uncontaminated reddish sand from a quarry near Glasgow (GQ, Garnock Quarry, Hugh King & Co Scotland, UK) was used as a 'control', whose mineralogical, chemical and physical properties are described in Comadran-Casas *et al.*<sup>40</sup>

### Soil hydrocarbon water extraction

Earlier studies have evidenced that only the fraction of substance (*i.e.*, PAH) dissolved in pore water is available to bacteria,<sup>36</sup> therefore in this study soil water extractions were used for the study of bacteria growth and ureolytic metabolic activity. Water extractions were deemed suitable to reduce the complexity of soil matrices. Water extractions containing soil hydrocarbons were obtained as follows: COV14 soil was sieved <2 mm in sterile conditions and stored in the fridge (4 °C) until further use. A soil extract containing extractable organic contaminants was obtained by placing COV14 soil and autoclaved ultrapure water (Milli-Q water filtration system Elga Purelab Chorus, from here onwards "DI") in a 100 mL borosilicate reagent glass bottle at a soil to liquid ratio of 1:2.5, topping it up to make sure no air remained in the bottle, mixed thoroughly, and placed in an orbital shaker at 200 rpm for 18 h. Subsequently, the sample was stored in the dark for 3 days for equilibration.<sup>41</sup> The soil extract was obtained by vacuum assisted filtration through 0.2 μm glass filter, obtaining a stock solution which was subsequently transferred to a reagent borosilicate glass bottle and stored in the fridge at 4 °C until further use. Glass bottles were previously rinsed thoroughly with deionised water, baked at 550 °C and autoclaved. A sample



of the 1 : 2.5 COV14 soil extract was analysed for total dissolved carbon. The soil extract was diluted 1 : 5, 1 : 10, 1 : 100 and 1 : 1000 with DI water to provide a range of hydrocarbon content.

### Glycine Max urease enzyme extraction

*Glycine Max* (soybean, Whole food earth, Kent, UK) beans were soaked overnight (>12 h) in DI water at a bean to water mass to volume proportion of 100 g L<sup>-1</sup>. The mixture was blended for 5 min and stirred for 30 min in an orbital shaker at 200 rpm. In sterile conditions, CaSO<sub>4</sub>·2H<sub>2</sub>O (>99.5% ACS reagent, Fisher Scientific) was added to the mixture at a 1 : 10 beans weight ratio, stirred for another 5 min, and allowed to rest for 1 h to induce solid coagulation. The mixture was then decanted into sterile 50 mL centrifuge tubes in sterile conditions and centrifuged at 3000 rpm overnight at 4 °C. The supernatant was subsequently filtered through 0.2 µm cellulose filter (Sartorius Minisart) into borosilicate glass bottles, obtaining a 100 g L<sup>-1</sup> stock urease enzyme solution, which was stored in the freezer (-20 °C) until further use. The 100 g L<sup>-1</sup> urease enzyme stock solution was diluted to 1 g L<sup>-1</sup> with DI water and stored in the freezer at -20 °C until use. Glass bottles were previously rinsed thoroughly with DI water, baked at 550 °C and autoclaved.

### Sporosarcina pasteurii culture

*S. pasteurii* DSM 33 was grown for 24 h in an orbital shaker incubator set at  $T = 30$  °C and 150 rpm in LBU media containing 10 g L<sup>-1</sup> tryptone (Formedium Ltd), 10 g L<sup>-1</sup> NaCl (≥99.0%, ACS reagent, Sigma Aldrich), 5 g L<sup>-1</sup> yeast extract powder (Formedium Ltd) and 20 g L<sup>-1</sup> urea (≥99.5% ACS reagent, Fisher Scientific) adjusted to pH 7 with NaOH and filter sterilised through 0.2 µm. Bacteria were pelleted by centrifugation at 30 min and 2500 g, resuspended in autoclaved 5 g L<sup>-1</sup> NaCl solution and diluted to OD<sub>600</sub> of 0.01 or 1. The optical density was measured at 600 nm with a spectrophotometer (DR 1900, Hach). This procedure was conducted daily prior to experimentation.

### Soil DNA extraction and detection of ureC gene

COV14 soil DNA was extracted with the RNeasy PowerSoil Total RNA Kit plus DNA Elution Kit (Qiagen) according to the manufacturer's instructions. PCR annealing temperature was optimised for target genes of bacterial ureolysis (*ureC*) using soil environmental DNA and tested on soil COV14 environmental DNA as template. Genes were amplified using primers listed in Table 1 with a HotStarTaq Polymerase kit (Qiagen) in a 50 µL final volume reaction composed of 5 µL 10× PCR buffer (15 mM MgCl<sub>2</sub>), 39.75

µL PCR water, 1 µL of each primer (10 µM, Eurofins), 1 µL dNTPs (10 µM each), 0.25 µL HotStarTaq DNA polymerase and 2 µL of DNA sample. PCR conditions were as follow: 95 °C for 15 min, (94 °C for 30 s,  $T_m^*$  °C for 30 s, 72 °C for 30 s) × 30 and 72 °C for 10 min, where  $T_m^*$  is the optimum annealing temperature determined through gradient PCR (Table 1) for each primer pair, and combined with agarose gel electrophoresis to separate PCR products.

### Soil urea hydrolysis through biostimulation and bioaugmentation

The potential to induce urea hydrolysis through biostimulation of soil autochthonous ureolytic bacteria was investigated in COV14 soil samples and on the uncontaminated quarry sand (GQ) serving as control. Samples were prepared by adding 2 g of soil (<2 mm) in sterile RNAase free 15 mL centrifuge tubes (Sarstedt AG&Co KG). Following preparation, 4 mL treatment solution were pipetted, and tubes were closed and thoroughly shaken to mix soil and solution, marking  $t = 0$ . Both sample preparation and treatment application were conducted in sterile conditions. The treatment solution was prepared adding 333 mM urea, 10 g L<sup>-1</sup> ammonium chloride (NH<sub>4</sub>Cl, >99.5% Acros Organics) and 3 g L<sup>-1</sup> nutrient broth (Nutriselect basic, Sigma Aldrich) to DI water, filter sterilised through sterile 0.2 µm cellulose syringe filters, transferred into pre-autoclaved borosilicate glass bottles in sterile conditions and stored at 4 °C until use. Samples were subsequently transferred into an incubator set at room temperature (20 ± 3 °C) with gentle shaking (150 rpm) and allowed to react in closed vials and dark conditions for up to 2 months. Samples were taken at reaction times ( $t_r$ ) = 0, 1, 2, 3, 4, 10, 20, 30 and 62 days. Three replicate samples were prepared for each reaction time point.

Bioaugmentation experiments were conducted on COV14 soil only. Soil samples were prepared as in biostimulation experiments. *S. pasteurii* was grown to an OD<sub>600</sub> = 1 and resuspended in sterile PBS buffer. Soils were treated with 2 mL of LBU media containing ×2 the mass proportion of chemical compounds and 2 mL of *S. pasteurii*. Samples were obtained at  $t_r = 0, 1, 2, 3$  and 7 days. Three replicate samples were prepared for each reaction time point.

Following reaction time, samples were centrifuged at 2500 g for 20 min to separate soil and solution. The solution was subsequently decanted and filtered through 0.2 µm for analysis of pH and NH<sub>4</sub><sup>+</sup>.

### Viability assay

To determine whether *S. pasteurii* could grow and maintain cell membrane structure in the presence of organic contaminants

**Table 1** List of *ureC* primers used in this study to test the presence of *ureC* gene in extracted environmental soil DNA and optimum annealing temperatures ( $T_m^*$ ) identified

Primer	Sequence (5' → 3')	Orientation	Length (bp)	Ref.	$T_m^*$ (°C)
ureC-F	AAGSTSCACGAGGACTGGGG	Forward	318	42	57
ureC-R	AGGTGGTGGCASACCATSAAGCAT	Reverse			
ureC-L2F	ATHGGYAARGCNGGNAAYCC	Forward	408	43	—
ureC-L2R	GTBSHNCCCCARTCYTCRTG	Reverse			
ureC607F	AARMTSCAYGARGACTGGGG	Forward	310	44	56
ureC898R	TGRCASACCATSAKCATGTCT	Reverse			



a viability experiment was conducted. *S. pasteurii* was grown overnight and diluted to an initial  $OD_{600} = 0.01$ .<sup>45</sup> Growth solutions were prepared by adding  $\times 2$  the mass proportion of chemical compounds of LBU media into soil extract solutions of increasing hydrocarbon concentration. Growth media were prepared in borosilicate glass bottles previously rinsed with DI water and baked at 550 °C and filter sterilised following preparation.

Equal volumes of *S. pasteurii* stock solution and growth solutions containing increasing concentration of hydrocarbons were pipetted to RNase free sterile 15 mL centrifuge tubes, mixed thoroughly, and placed in an orbital shaker incubator at 150 rpm and  $T = 30$  °C. Samples were obtained at  $t_r = 0, 2, 4, 8, 12, 20$  and 24 h. Sampling was destructive such that three biological replicates were prepared for each hydrocarbon concentration and reaction time point.

Methods to study bacteria growth and kinetics have typically involved optical density or cell dry weight<sup>46</sup> which are indirect measurements of cell concentration and can be misleading when trying to determine bacteria viability nor provide information on cell membrane stability.<sup>47,48</sup> In this study we employed flow cytometry which provides direct measurement of total cell counts and has been used to differentiate total from intact cell counts through the use of stains that penetrate or not, respectively, cell membranes, from which cell viability and membrane structure can be inferred.<sup>49,50</sup>

Quantification of bacteria population was performed using the Cytotflex flow cytometer (Beckman Coulter). Samples were prepared by cell fixation with glutaraldehyde (1% in DI water) and diluted as necessary with filtered (0.2  $\mu\text{m}$  Sartorius™ Minisart™ Plus Syringe Filters, Fisher scientific) DI water.<sup>51</sup> Samples were stained for total and intact cell count with 10  $\mu\text{L mL}^{-1}$  of SYBR Green I (SGI) and 10  $\mu\text{L mL}^{-1}$  of SYBR Green I mixed with propidium iodide (SGI/PI), respectively, and incubated in the dark for 15 min before measurement. The total cell stain was prepared by diluting the stock solution of SGI (10 000 $\times$  in DMSO, Thermofisher) 1 : 100 in EDTA (1 mM) and the intact cell stain by mixing SGI with PI (1.6 mM) and diluting 1 : 100 in EDTA (1 mM) for a final concentration of 0.6 mM PI and 100 $\times$  for SGI. Gating was used to distinguish the selected bacteria population background with the aid of negative controls consisting of the DI water used for dilutions, growth solutions composed of LBU in soil extracts and filtered samples (<0.2  $\mu\text{m}$ ) to remove any bacterial cells using the software CytExpert (Beckman Coulter).

The bacteria specific growth rate was estimated by fitting a regression line to the logarithmic cell counts during the exponential growth phase, with the slope of the line representing the growth rate. The lag phase duration was estimated as the x-axis intercept of the regression line, assuming a theoretical extrapolation from the exponential phase.<sup>52</sup>

### Urease activity assay

To investigate the hydrocarbon contaminant effect on urease activity at enzyme and cell level, extracted *Glycine Max* urease (1 and 100  $\text{g L}^{-1}$ ) and *S. pasteurii* ( $OD_{600} = 0.01$  and 1) were exposed to increasing concentrations of COV14 soil extracts containing 666 mM urea at a 1:1 volume ratio. The higher

enzyme and cell concentrations were chosen for comparative purposes with previous studies providing similar enzyme and cell urease activity rates.<sup>52,53</sup> Positive controls included *Glycine Max* urease and *S. pasteurii* exposed to solutions containing no contaminants but 666 mM urea or 666 mM urea plus 5  $\text{g L}^{-1}$  NaCl, respectively. Negative controls were run on 666 mM urea solution, COV14 extracts containing 666 mM urea, and 666 mM urea plus 5  $\text{g L}^{-1}$  NaCl, where *Glycine Max* urease or *S. pasteurii* solutions were replaced by DI water.

The urease activity (UA) was determined through changes in electrical conductivity (EC) over time with measurements taken every 0.5 min over 20 min<sup>54</sup> by adding equal volumes of either *Glycine Max* urease or *S. pasteurii* and COV14 soil extracts plus urea in glass vials. Measuring urea hydrolysis with electrical conductivity (EC) is useful because urea hydrolysis produces ions ( $\text{NH}_4^+$  and  $\text{HCO}_3^-$ ), which increase the solution's ability to conduct electricity and thus EC serves as a direct measurement of ureolysis. Glass vials previously rinsed with DI water and baked at 550 °C overnight. The UA was computed as:

$$UA(\mu\text{M min}^{-1}) = \frac{\Delta\text{EC}}{\Delta t} f \quad (6)$$

where  $f = 22.2$  is a conversion factor of EC to urea hydrolysed (11.1) divided by the 1 : 2 dilution factor in urea concentration.<sup>54</sup> The slope and standard error of the measured changes in EC over time was computed through a linear regression with the data points of the three replicate runs.

### Chemical analyses

**pH.** Solution pH was measured with a pH meter (Orion Star A215, Thermo Scientific) probe (Orion ROSS Ultra SM 103BNUWP, Thermo Scientific), calibrated to three points (pH = 4, 7 and 10, Orion Application Solution, Thermo Scientific).

**Ammonium ( $\text{NH}_4^+$ ).**  $\text{NH}_4^+$  in solution was analysed with an ammonium cuvette test (100–1800  $\text{mg L}^{-1}$   $\text{NH}_4\text{-N}$ , LCK502, Hach UK) and spectrophotometer (DR 1900, Hach UK) according to the manufacturer instructions.

**Electrical conductivity (EC).** Solution EC was measured with an EC meter (Orion 5 Star, Thermo Scientific) probe (Orion 013605MD, Thermo Scientific) calibrated to 1413 and 12 880  $\mu\text{S cm}^{-1}$  buffer solutions (Orion Application Solution, Thermo Scientific).

**Soil total carbon.** COV14 soil total carbon and isotopic  $\delta^{13}\text{C}$  composition were analysed with a Picarro Combustion Module Cavity Ring-Down Spectroscopy (CM-CRDS) system (CM by NC Technologies, G2201-i CDRS) interfaced by a Caddy Continuous Flow Interface (A2100) on five analytical replicates.

**Soil total and exchangeable elemental composition.** The total elemental composition COV14 soil was carried out through a triacid hotplate digestion at the Scottish University Environment Research Centre (SUERC, East Kilbride, G75 0QF, Scotland, UK) in triplicate. Soil samples were consecutively digested overnight on a hotplate at 120 °C, first with HF +  $\text{HNO}_3$ , secondly with  $\text{HNO}_3$ , and finally with HCl. Elements Al, Ba, Ca, Fe, K, Mg, Mn, Na, Sr, Ti and Zn were determined by inductively coupled plasma-optical emission spectrometry (ICP-OES,



Thermo Scientific iCap 7000) and As, B, Cd, Co, Cr, Cu, Li, Mo, Ni, Pb, Sb, Sn and V by ICP-mass spectrometry (ICP-MS, Agilent 7500ce). ICP-MS was used due to the higher limit of detection over ICP-OES according to SUERC internal laboratory procedures.

The elemental composition of the soil exchangeable fraction was determined on three analytical replicates through the first step of the Tessier *et al.*<sup>55</sup> sequential extraction. In summary, 1 g of soil and 8 mL of 1 M MgCl were mixed for 1 h at room temperature. The solution containing soil exchangeable elements was obtained through centrifugation, decantation, filtration (0.2  $\mu\text{m}$ ), and acidification with HNO<sub>3</sub>. Elements Na, K, Mg, Ca, Sr, Ba, Ti, V, Cr, Mo, Mn, Fe, Co, Ni, Cu, Zn, Cd, B, Al, Si, Sn, Pb, As, Sb, S, Se were determined by ICP-OES (Agilent 5900 SVDV).

**Total dissolved organic carbon in soil extracts.** The total dissolved organic carbon of the 1:2.5 COV14 soil extract was determined on three analytical replicates with a total organic carbon analyser (TOC-L, Shimadzu) calibrated to 2.5 and 5 ppm potassium phthalate monobasic (>99.5%, Sigma Aldrich).

## Results and discussion

### Soil characterisation

The hydrocarbon polluted COV14 soil was composed of 70% sand,  $7.9 \pm 0.3\%$  silt and  $4.7 \pm 0.2\%$  clay size-particles (Table S1). The moisture content was determined at 23%. The total carbon and isotopic composition of <sup>13</sup>C were  $8 \pm 4\%$  and  $-26.4 \pm 0.4\%$ , respectively ( $n = 5$ ) (Table S2). The soil total elemental analysis indicated Pb ( $490 \pm 30 \text{ mg kg}^{-1}$ ), Mn ( $460 \pm 50 \text{ mg kg}^{-1}$ ), Ba ( $470 \pm 50 \text{ mg kg}^{-1}$ ), Cu ( $240 \pm 90 \text{ mg kg}^{-1}$ ) and Zn ( $310 \pm 20 \text{ mg kg}^{-1}$ ) were present in significant concentrations (Fig. S2A). Of these, only Mn ( $28 \pm 3 \text{ mg kg}^{-1}$ ) and Ba ( $10 \pm 3 \text{ mg}$

$\text{kg}^{-1}$ ) were present at concentrations  $>5 \text{ mg kg}^{-1}$  in the soil exchangeable fraction (Fig. S2B). The analysis of soil PAH indicated presence of phenanthrene ( $28.7 \pm 0.2 \text{ mg kg}^{-1}$ ), fluoranthene ( $18.4 \pm 0.2 \text{ mg kg}^{-1}$ ) and pyrene ( $16.0 \pm 0.1 \text{ mg kg}^{-1}$ ). Additionally, anthracene, fluorene, benzo(a)anthracene, benzo(b)fluoranthene, acenaphthylene ( $5\text{--}10 \text{ mg kg}^{-1}$ ) and naphthalene, chrysene, benzo(k)fluoranthene, benzo(a)pyrene, indeno(1,2,3-*cd*)pyrene, dibenzo(a,h)anthracene and benzo(g,h,i)perylene were quantified ( $1\text{--}5 \text{ mg kg}^{-1}$ ) (Fig. S3). These results confirmed presence of both organic and inorganic pollutants in COV14 soil.

### Soil genetic potential for ureolysis

The extracted RNA in COV14 soil confirmed the soil was biologically active (Fig. 1A). Bacterial *ureC* genes relevant in the bioremediation of heavy metals through microbial-induced calcite precipitation<sup>2-12</sup> were evidenced in both the uncontaminated GQ soil and the PAH contaminated COV14 soil in extracted environmental DNA samples (Fig. 1B and C). The presence of *ureC* was confirmed by the amplification of a PCR product with the expected size of 318 bp<sup>42-44</sup> indicating the soils' potential for ureolysis. Of the *ureC* primers tested, the primer by Collier *et al.*<sup>42</sup> provided the best results, binding to the DNA *ureC* gene and *ureC* standard over a temperature range 50–61 °C (Fig. S5). The ureC607F&898R pair<sup>44</sup> provided good results binding to DNA and *ureC* standard over 56–62 °C with strongest bands showing at 56 °C (Fig. S7), whilst the ureC 2LF&R primer<sup>43</sup> did not bind to DNA nor *ureC* standard at any of the annealing temperatures tested (56–68 °C) (Fig. S6).

### Ureolytic activity of soil autochthonous ureolytic microorganisms

Biostimulation of urea hydrolysis in the uncontaminated quarry sand (GC) used as control was evidenced by increases in NH<sub>4</sub><sup>+</sup>

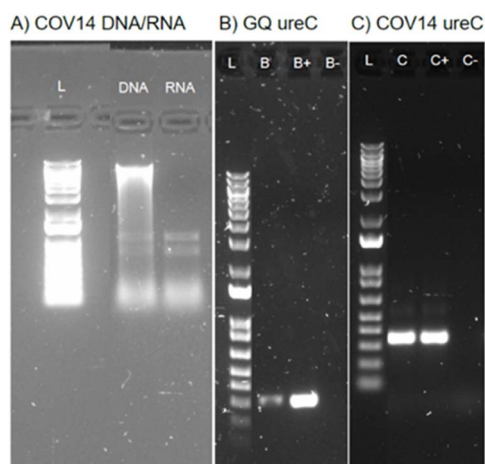


**Fig. 1** (A) Extracted DNA and RNA from soil COV14. (B and C) PCR results showing presence of *ureC* genes in DNA extracted from (B) GQ and (C) COV14 soil. Column well IDs without, with plus (+) and negative (–) signs indicate environmental DNA sample, environmental DNA sample spiked with 1  $\mu\text{L}$  *ureC* standard and control PCR water, respectively. “L” stands for ladder used to estimate the base pair (bp) length of the target gene. *ureC* primers used developed by Collier *et al.*<sup>42</sup>

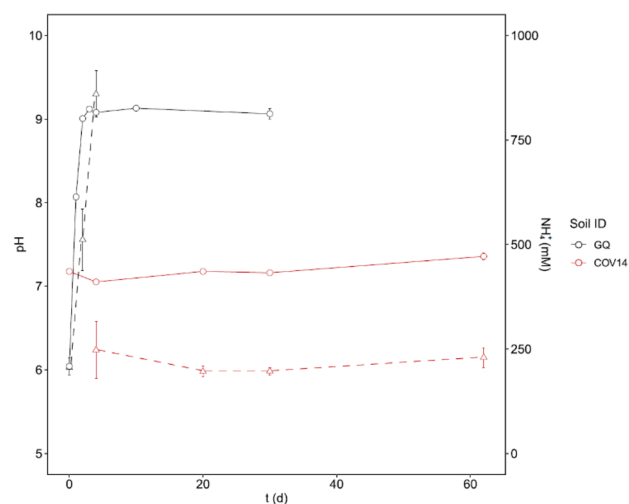


**Fig. 2** Evolution of soil pH (left y-axis, circle) and NH<sub>4</sub><sup>+</sup> (right y-axis, triangle) over time following application of treatment to induce urea hydrolysis on an uncontaminated quarry sand (GQ) and a polluted soil from a gas plant (COV14). Markers and error bars indicate the average and standard deviation of three replicate samples.



( $205 \pm 5$  to  $859 \pm 54$  mM) and pH ( $6$  to  $9 \pm 0.01$ ) within two days (Fig. 2). The increase in  $\text{NH}_4^+$  ( $\Delta\text{NH}_4^+ = 654$  mM) indicated all urea applied ( $333$  mM) had been hydrolysed, according to the stoichiometry of the urea hydrolysis reaction (eqn (1)). From this we estimated an urease activity of  $227 \mu\text{M urea min}^{-1}$  until consumption of all urea. Urea hydrolysis induces an increase in soil pH and  $\text{NH}_4^+$  due to excess  $\text{OH}^-$  resulting from equilibration of  $\text{CO}_2$  and  $\text{NH}_3$  derived from urea hydrolysis with water (eqn (2)) and ((3)). It should be noted that the urease activity is an estimation since  $\text{NH}_4^+$  ions easily sorb to soil matrices and  $\text{NH}_4^+$  begins to deprotonate to ammonia ( $\text{NH}_3$ ) (gas) at pH  $\sim 7.4$ , reaching equilibrium at  $\text{p}K_a = 9.25$ . This causes degassing of  $\text{NH}_3$  from the system which we did not quantify.

The same treatment application to COV14 soil did not result in significant changes in pH ( $7.1$ – $7.4$ ) or  $\text{NH}_4^+$  ( $205$  mM) over 62 days (Fig. 2), indicating urea hydrolysis in the polluted soil (COV14) did not occur to a measurable extent. Despite the COV14 and GQ soils are of different nature, mineralogical and physicochemical composition and thus cannot not strictly serve as control, the GQ soil illustrated the classic ureolysis response to urea application by autochthonous ureolytic soil bacteria in absence of potential inhibitors of ureolysis (e.g., pollutants), thus serving as a reference. Given the presence of *ureC* genes indicating COV14 soils' genetic potential for urea hydrolysis

(Fig. 1), the absence of urea hydrolysis could be attributed mainly to the presence of soil contaminants.

Heavy metals are known inhibitors of urea hydrolysis in soils. The strength of inhibition follows the order  $\text{Hg}^{2+} \approx \text{Ag}^+ > \text{Cu}^{2+} \gg \text{Ni}^{2+} > \text{Cd}^{2+} > \text{Zn}^{2+} > \text{Co}^{2+} > \text{Fe}^{3+} > \text{Pb}^{2+} > \text{Mn}^{2+}$ .<sup>56–58</sup> The concentration of Mn and Ba in COV14 exchangeable fraction was determined at  $28 \pm 3$  and  $10 \pm 3$   $\text{mg kg}^{-1}$ , respectively, equivalent to soil-solution concentrations of  $0.5 \pm 0.1$  and  $0.07 \pm 0.02$  mM. The rest of elements in the COV14 soil exchangeable fraction were  $<0.02$  mM. The elements present in COV14 extracts were hence not among the strongest element inhibitors. Urea hydrolysis inhibition in pure cultures of *S. pasteurii* has been observed at  $\text{Mn} = 50$   $\text{mM}$ <sup>59</sup> although the minimum inhibitory concentration remains undetermined. For Ba, no data exist yet to our knowledge in pure cultures. Inhibitory concentrations of urea hydrolysis vary across elements and bacterial species<sup>40</sup> however, studies on pure cultures indicate minimum inhibitory concentrations are typically one to three orders of magnitude higher than  $0.02$  mM.<sup>6,60–63</sup> Biostimulation of urea hydrolysis was not hindered in a soil containing Mn and Ba concentrations in the exchangeable fraction ( $10 \pm 1$  and  $33 \pm 1$   $\text{mg kg}^{-1}$ ) similar to COV14.<sup>40</sup> It was therefore concluded that elements present in the exchangeable fraction at the

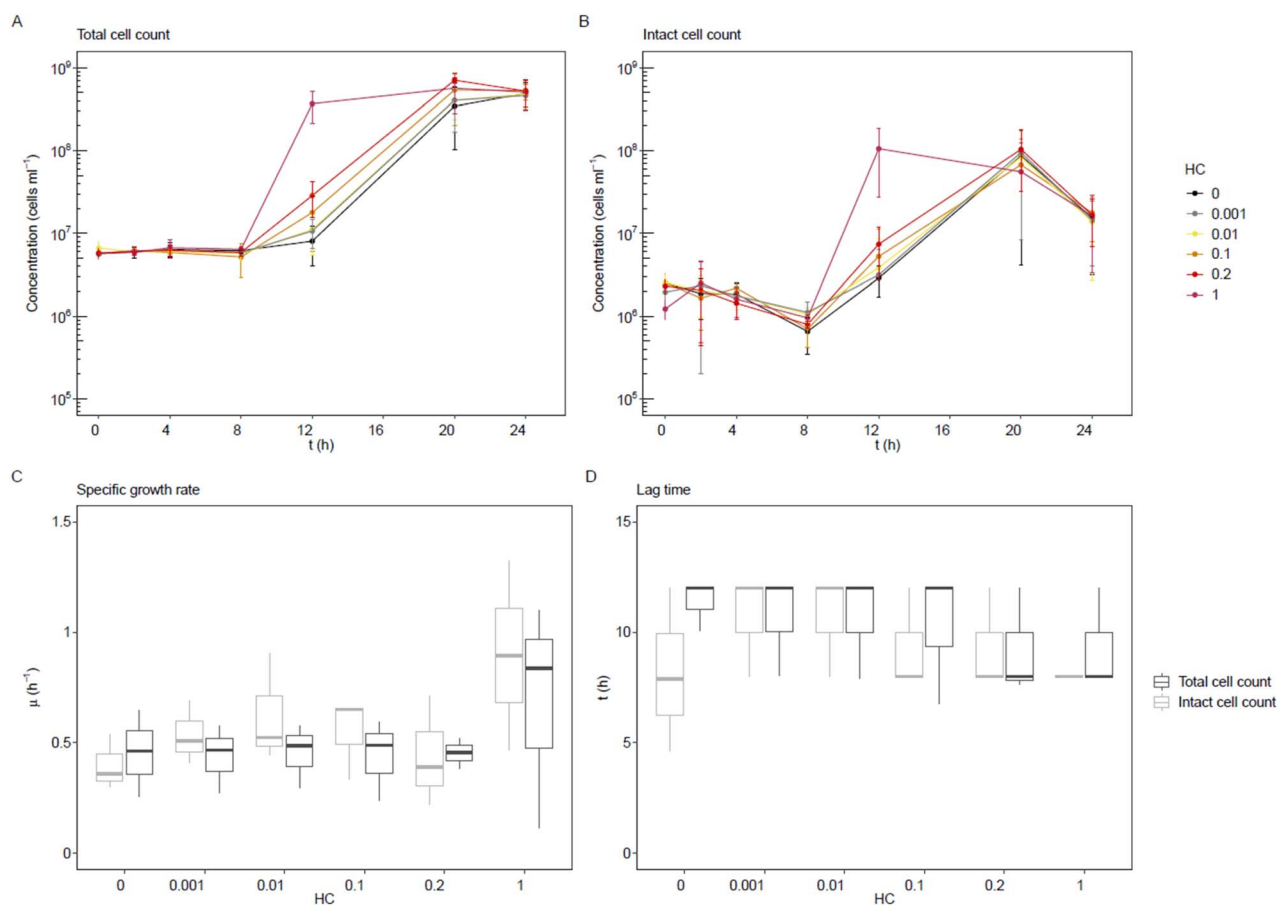


Fig. 3 Growth curve and kinetics of *S. pasteurii* (cells  $\text{mL}^{-1}$ ) population over 24 hours with different dilutions of hydrocarbon. Flow cytometry is used to measure the (A) total and (B) intact cell count. (C) Growth rate ( $\text{h}^{-1}$ ) and (D) lag time (h) of the intact and total cell count is calculated using the slope and intercept. Markers and error bars indicate the average and standard deviation of three biological replicate samples.



concentrations determined were not the main cause of urea hydrolysis inhibition in COV14 soil.

Organic contaminants can have both stimulatory and inhibitory effects on soil urea hydrolysis. Increases in urease activity have been observed at PAH  $< 2 \text{ mg kg}^{-1}$ <sup>27</sup> and specifically  $< 1 \text{ mg kg}^{-1}$  naphthalene and phenanthrene,<sup>23</sup> attributed to utilisation of organic contaminants as carbon sources by autochthonous microorganisms resulting in increased microbial counts, soil respiration, biomass, and enzyme activities.<sup>23</sup> On the contrary, sharp reductions in urease activity have been observed at total petroleum hydrocarbon (TPH)  $> 300 \text{ mg kg}^{-1}$ ,<sup>28</sup> and in the combined presence of PAH (phenanthrene, fluoranthene, benzo(a)pyrene;  $0.01\text{--}3.2 \text{ mg kg}^{-1}$ ) and heavy metals (Cd, Zn, Pb).<sup>30</sup> Inhibitory effects have been attributed to suppression of the microbial populations involved in the N, P, or C cycles,<sup>28</sup> prevention of enzyme activity expression due to interaction of organic contaminants with cell surfaces<sup>29</sup> and changes in the enzyme molecular structure active site caused by heavy metal interactions and enzyme denaturation by PAH.<sup>30</sup> The measured PAH in COV14 added up to  $116 \text{ mg kg}^{-1}$ , an order of magnitude higher than PAH concentrations observed to decrease urea hydrolysis rates (PAH  $\sim 2 \text{ mg kg}^{-1}$ ).<sup>27,30</sup> Biostimulation of urea hydrolysis by COV14 soils' autochthonous ureolytic bacteria was thus likely inhibited by PAH.

### Viability of *Sporosarcina pasteurii* in the presence of hydrocarbons

Hydrocarbon mediated inhibition of urea degradation may be the result of negative effects on bacteria growth and enzyme activity. To assess whether ureolytic bacteria could grow in the hydrocarbon polluted soil environment, we used flow cytometry to quantify *S. pasteurii* total and intact cell counts over the course of 24 hours and determine growth kinetics under increasing concentration of hydrocarbons.

The growth of *S. pasteurii* followed the typical bacteria growth pattern distinguished by a lag, exponential growth, stationary, and decline phases (Fig. 3A). The presence of hydrocarbons had no significant effect on the growth parameters compared to control (HC = 0;  $p > 0.05$ ). The specific growth rates determined from the exponential phase of the total cell count remained consistent across hydrocarbon concentrations (ranging from  $0.44$  to  $0.46 \text{ h}^{-1}$ ), except at the highest hydrocarbon concentration where a notable increase (HC 1 =  $0.68 \pm 0.51 \text{ h}^{-1}$ ) was determined (Fig. 3C). Although this indicated a potential enhancement in growth, differences in specific growth rate were not statistically different ( $p = 0.97$ ). Similarly, there were no significant differences in lag time in the presence of hydrocarbons compared to control for both intact ( $p = 0.4$ ) and total ( $p = 0.89$ ) cell count (Fig. 3D). This demonstrated the bacteria's ability to acclimatise to the new environment was not affected by the presence of hydrocarbons and that bacteria were readily able to utilise the carbon sources in the media.

Hydrocarbons can be toxic to bacteria reducing the growth rate by causing membrane damage.<sup>64</sup> The total and intact cell counts after 24 hours ( $\sim 5 \times 10^8 \text{ cells mL}^{-1}$  for total cell count,  $p = 0.86$ ;  $\sim 1.6 \times 10^7 \text{ cells mL}^{-1}$  for intact cell count) were not

significantly different across samples ( $p = 0.89$ , Fig. 3A and B). Results further indicated that at least 2% of the total measured bacteria had an intact and undamaged cell membrane after 24 h. Future studies could incorporate analysis of metabolites leaked from cells due to membrane damage by PAH to better understand the effect of PAH in intact cell count. Added to the insignificant differences observed in lag and growth rate phases, it was concluded that *S. pasteurii* was able to grow successfully in the presence of hydrocarbons and there was no significant difference in bacteria numbers and cell viability after 24 h, regardless of presence of hydrocarbons at the concentrations tested.

Despite there being no significant increase in specific growth rate results indicate *S. pasteurii* grew faster in the polluted soil environment than in LBU media. Since LBU media was constant across tested solutions and the only difference across treatment media was the organic carbon dissolved from soil during the water extraction procedure, this indicated *S. pasteurii* could be utilising additional carbon sources for growth. It has been argued that PAH (phenanthrene, anthracene, fluoranthene, pyrene, benzo[a]anthracene and chrysene) can be easily used by the soil microorganisms as a source of carbon and energy,<sup>65,66</sup> were low toxicity, three-ring PAH, are decomposed more easily by microorganisms than five-ring PAH.<sup>67</sup> Notably, the ureolytic bacteria *Pseudomonas aeruginosa* N6P6 has been shown to utilise PAH as a sole source of carbon,<sup>68</sup> indicating this could be a common trait across ureolytic bacteria. Another contributing factor is that dissolved organic matter extracted from the soil along with PAH offered additional carbon sources and a protection mechanism. Higher soil organic matter has been found to decrease the negative effects of PAH on soil urease activity<sup>27,69</sup> attributed to sorption of organic pollutants to soil organic matter.<sup>70,71</sup> In this study we did not elucidate whether *S. pasteurii* used hydrocarbons, other dissolved organic carbon from soil or compounds in LBU media as source of carbon. The presence of only one lag and exponential phase indicated bacteria did not show a diauxic growth and therefore used one preferred carbon source<sup>64</sup> however the datapoints in the exponential growth phase are limit this interpretation. Further studies including analysis of hydrocarbon characterisation through gas-chromatography-mass spectrometry<sup>39</sup> are recommended to elucidate whether changes in PAH composition indicative of urea degradation occurred during growth.

### Urease activity of *Glycine Max* urease and *Sporosarcina pasteurii* in the presence of hydrocarbons

To establish whether organic contamination and PAH in particular inhibited urea hydrolysis, we investigated both the urease activity of *Glycine Max* and *S. pasteurii* in the presence of increasing concentrations of COV14 soil water extracts. The total organic carbon of the undiluted soil water extract (referred to as HC = 1) was determined at  $70 \pm 0.7 \text{ mg L}^{-1}$  ( $n = 3$ ).

**Urease activity in absence of contaminants.** The urease activity of *Glycine Max* at 1 and  $100 \text{ g bean L}^{-1}$  in absence of contaminants was determined at  $114 \pm 7$  and  $4521 \pm 304 \mu\text{mol urea min}^{-1}$  (HC = 0, Fig. 4A) and the *S. pasteurii* urease activity



at  $OD_{600} = 0.01$  and 1 at  $30 \pm 9.6$  and  $2102 \pm 26$   $\mu\text{mol urea min}^{-1}$  (HC = 0, Fig. 5A), respectively. The urease activities at the higher dosages of enzyme (100 g bean  $L^{-1}$ ) and cell ( $OD_{600} = 1$ ) were comparable to values reported in the literature by Weng *et al.*<sup>53</sup> ( $\sim 4.2$  mM urea  $min^{-1}$ ) and Minto *et al.*<sup>52</sup> ( $\sim 3.7$ – $4.6$  mM urea per min per  $OD_{600}$ ), respectively, but significantly lower than values reported by Liu *et al.*<sup>72</sup> for *Glycine Max* ( $\sim 10$  mM urea  $min^{-1}$ ) and Lauchnor *et al.*<sup>73</sup> for *S. pasteurii* ( $1.93$  mM urea  $min^{-1}$  at  $OD_{600} = 0.025$ ). The variation in urease activity of *Glycine Max* could arise from the grinding process (e.g., particle size of ground beans or inactivation of enzyme if temperature during grinding exceeded  $T > 65$  °C Pettit *et al.*<sup>74</sup>) and the temperature at which EC conductivity is measured. Another cause for discrepancy at the higher dosages could be the lower urea concentration used in this study of 666 mM compared to 1.1  $M$ <sup>54</sup> which may have been insufficient to

saturate the enzyme and thus reach maximum reaction kinetics ( $v_{max}$ ).

The measured urease activity of *S. pasteurii* was 2 to 3.7 times lower than that of *Glycine Max*. At equivalent amounts of enzyme, the reported urease activity of *S. pasteurii* is significantly higher than that of *Glycine Max* (2500 vs. 650–800  $\mu\text{mol urea min}^{-1} \text{mg}^{-1}$  enzyme, respectively),<sup>38</sup> indicating the amount of urease obtained with 1 and 100 g  $L^{-1}$  *Glycine Max* and  $OD_{600} = 0.01$  and 1 *S. pasteurii* were not equivalent.

The measured urease activities of *Glycine Max* urease and *S. pasteurii* were not proportional to their respective concentrations. Instead of the  $\times 100$  factor in urease activity expected from dilution, the difference in urease activity obtained with the lower and higher enzyme and cell dosages were  $\times 36$  and  $\times 40$ , respectively. This was in contrast to the reported proportionality between urease activity and concentration of *Glycine Max* within 20–100 g  $L^{-1}$ ,<sup>72</sup> and *S. pasteurii* cell within  $OD_{600} = 0.025$ – $0.15$ .<sup>73</sup>

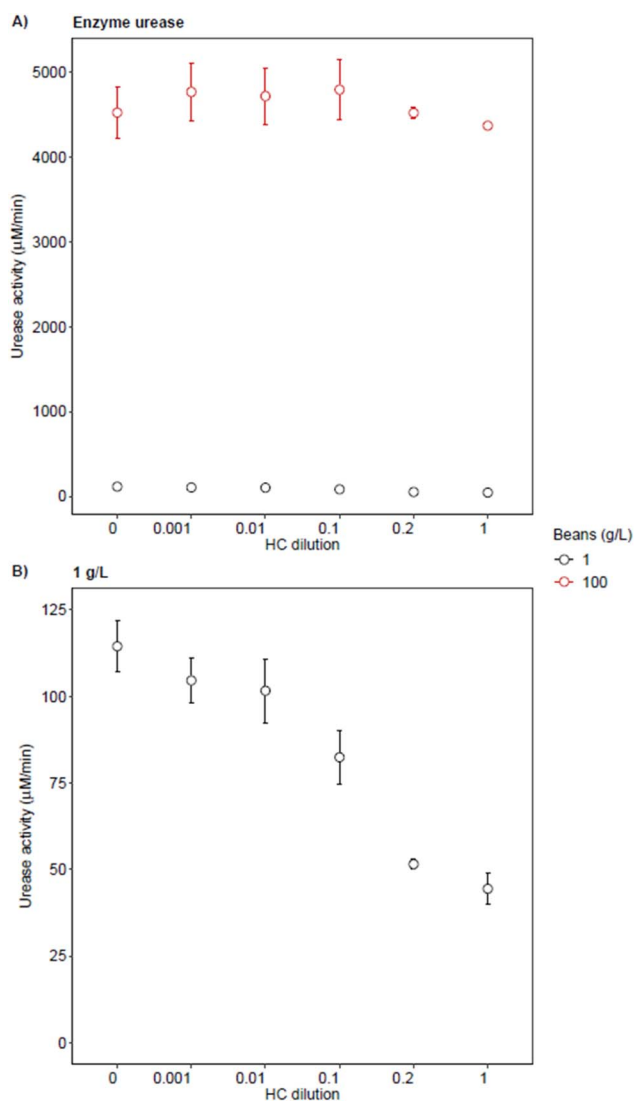


Fig. 4 Urease activity of *Glycine Max* urease in presence of hydrocarbons (HC) extracted from soil COV-14. (A) *Glycine Max* urease concentration of 1 and 100 g  $L^{-1}$ ; (B) *Glycine Max* urease concentration of 1 g  $L^{-1}$ . Markers and error bars indicate average and standard deviation of three replicate tests.

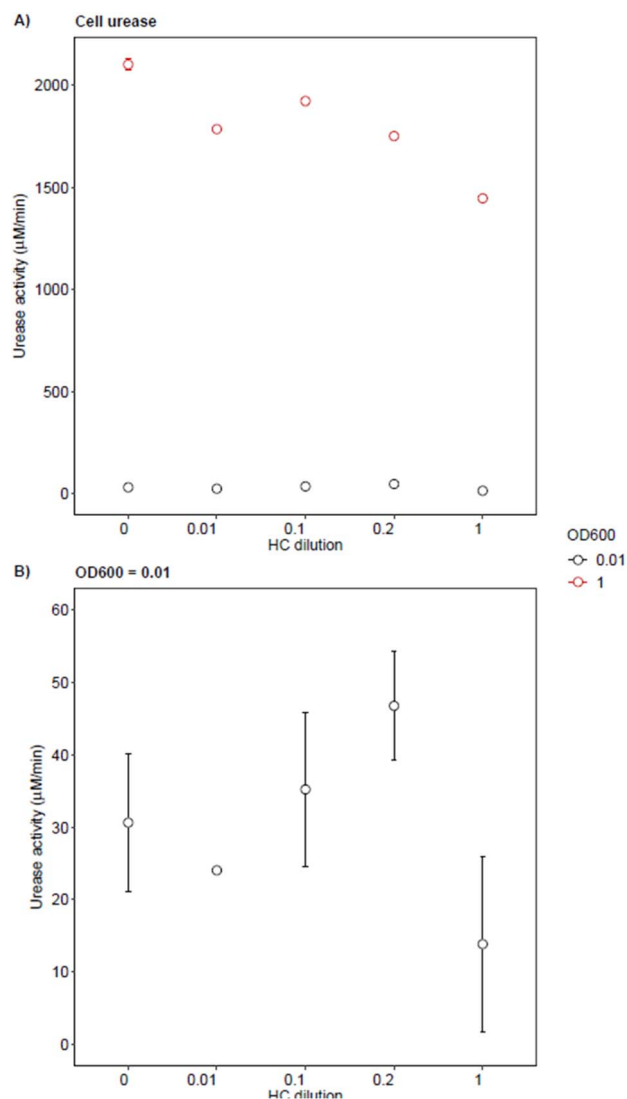


Fig. 5 Urease activity of *S. pasteurii* in presence of hydrocarbons (HC) extracted from soil COV-14. (A) *S. pasteurii* cell  $OD_{600} = 0.01$  and 1; (B) *S. pasteurii* cell  $OD_{600} = 0.01$ . Markers and error bars indicate average and standard deviation of three replicate tests.



and was attributed to insufficient urea to reach  $v_{\max}$  at the higher dosages of enzyme and cell.

**Effect of hydrocarbons on enzyme urease activity.** At both 1 and 100 g L<sup>-1</sup>, *Glycine Max* urease activity was quantifiable at all hydrocarbon concentrations (Fig. 4A). At 100 g L<sup>-1</sup>, no significant differences in urease activity were determined at any hydrocarbon concentration ( $p = 0.88$ ) (Fig. 4A). Instead, at 1 g L<sup>-1</sup> urease activity decreased significantly with increasing hydrocarbon concentration ( $p = 4 \times 10^{-5}$ ) (Fig. 4B), evidencing inhibition by hydrocarbons at enzyme level. A significant decrease in urease activity was determined at TOC  $\geq 3.5 \pm 0.1$  mg L<sup>-1</sup> (i.e., HC  $\geq 0.1$ ). At the highest hydrocarbon concentration (TOC = 35 mg L<sup>-1</sup>, HC = 1), urease activity was 61% lower than in absence of contaminants (HC = 0). We do not know of any earlier studies on the effect of PAH on enzyme urease activity relevant for comparison with these results, however our results clearly evidenced urease activity inhibition was dependant on enzyme and pollutant concentration, suggesting the mechanism of inhibition at enzyme level was competitive. To further investigate urease enzyme inhibition by hydrocarbons, future *in vitro* studies to elucidate changes in enzyme structure in the presence of pure enzyme and chemicals are encouraged.

**Effect of hydrocarbons on cell urease activity.** Urease activity of *S. pasteurii* at OD<sub>600</sub> = 1 was quantified at all hydrocarbon concentrations tested (Fig. 5A). Presence of hydrocarbons had a significant effect on cell urease activity ( $p = 5 \times 10^{-5}$ ). A significant decrease in cell urease activity was determined at the lowest hydrocarbon concentration tested (HC  $\geq 0.01$ , TOC =  $0.7 \pm 0.1$  mg L<sup>-1</sup>, Fig. 5A), resulting in a 31% slowdown in urease activity at the highest hydrocarbon concentration (HC = 1, TOC = 35 mg L<sup>-1</sup>). Similar to the effects observed in the enzyme assays, the results at OD<sub>600</sub> = 1 evidenced an inhibitory effect of hydrocarbons on cell urease activity which was dependant on pollutant and cell concentration. At OD<sub>600</sub> = 0.01, cell urease activity was determined <60  $\mu\text{M min}^{-1}$  at all hydrocarbon concentrations tested (Fig. 5B). Changes in electrical conductivity over time at OD<sub>600</sub> = 0.01 were hardly detectable over the 20 min experiment, resulting in linear regressions with slopes ranging from 0.6–1.6  $\pm 0.03$ –0.48  $\mu\text{S cm}^{-2} \text{min}^{-1}$  which were not significantly different than controls without cells ( $-1.8$ –2.2  $\pm 0.2$   $\mu\text{S cm}^{-2} \text{min}^{-1}$ ). Therefore, it was concluded that cell urease activity at OD<sub>600</sub> = 0.01 was either below detection limits or was inhibited altogether, such that the effect of hydrocarbons on urease activity could not be elucidated.

Contrary to the enzyme assay, inhibition was readily observed at the highest cell (OD<sub>600</sub> = 1) and lowest contaminant concentration (TOC = 0.35 mg L<sup>-1</sup>), suggesting PAH had a stronger inhibitory effect at cell than enzyme level. This could be because the amount of enzyme urease in *Glycine Max* and *S. pasteurii* solutions were not equivalent, as indicated from urease activities obtained in absence of contaminants. Additionally, the *Glycine Max* solution contained an undetermined amount of dissolved organic matter (<0.2  $\mu\text{m}$ ) which could bind to PAH<sup>27,75</sup> and decrease its inhibitory effect. Future experiments with pure urease extract and equivalent and normalised

urease enzyme concentrations would be necessary to elucidate differences in strength of inhibition at enzyme and cell level.

It has been suggested PAH have a non-specific narcotic mode of action on bacteria.<sup>34,35</sup> This narcotic mode of action has been observed in soil nitrifiers, where nitrification rates decreased proportionally to PAH lipophilicity,<sup>36</sup> suggesting cells might be exposed to a combined inhibitory effect occurring at cell and enzyme level. The urea hydrolysis assay revealed that cell (OD<sub>600</sub> = 1,  $\sim 10^9$  cells mL<sup>-1</sup>; Fig. 5) and enzyme (1 g L<sup>-1</sup>) urease activity were significantly impeded with increasing hydrocarbon concentration, suggesting urea hydrolysis was largely inhibited at the low initial cell concentration used in the growth experiment (OD<sub>600</sub> = 0.01,  $\sim 10^6$  cells mL<sup>-1</sup>) (Fig. 3). Based on present extensive literature on urease inhibitors,<sup>38,76</sup> we did not consider inhibitors were among media (e.g., urea itself, or byproducts of urea hydrolysis, NH<sub>4</sub><sup>+</sup>) but rather on extracted soil compounds. However, we do not discard the alkaline pH and byproducts of ureolysis could have caused changes in soil extract compounds (humic and fluvic acids, PAH) that may have influenced the results. The fact that the lag and exponential growth phases did not show any significant differences across hydrocarbon concentrations thus indicated bacteria used carbon sources other than urea for growth. In addition, the lack of apparent negative effects on cell growth and cell membrane stability (Fig. 3) indicated the negative effects on cell urease activity with increasing hydrocarbon concentration were primarily due to negative effects on the enzyme urease rather than the overall cell function. Future studies on functional gene expression during growth would help elucidate whether bacteria are synthesising urease during the initial growth stages and/or are utilising other sources of carbon.

### Bioaugmentation of urea hydrolysis with *Sporosarcina pasteurii*

Based on the successful growth and urease activity of *S. pasteurii* in the COV14 soil extract containing hydrocarbons (Fig. 3A and 5), we conducted a bioaugmentation experiment in COV14 soil with *S. pasteurii* at OD<sub>600</sub> = 1. Following inoculation of *S. pasteurii* and urea on COV14 soil, pH increased from 7.5 to 9 in the first 24 h and remained stable for 7 days. Similarly, NH<sub>4</sub><sup>+</sup> increased from  $20 \pm 1$  to  $515 \pm 19$  mM within the first day, remaining stable until the end of the experiment, equivalent to 77% urea hydrolysed (Fig. 6). These results were consistent with the urea hydrolysis reaction and the reaction time necessary by indigenous bacteria to hydrolyse urea in the uncontaminated GQ sand (Fig. 2) and literature,<sup>17,19–21</sup> confirming that at sufficient cell concentration feasibility of urea hydrolysis by *S. pasteurii* in soil environments polluted by PAH via bioaugmentation. It should be noted that the treatment media for biostimulation and bioaugmentation experiments were NBU and LBU, respectively, which could make the results less comparable. We used LBU to grow *S. pasteurii* because we observed a faster growth in our preliminary experiments (no data available). Both are complex non-selective liquid media used for growing bacteria and have been used as non-specific media to successfully induce ureolysis in polluted soils: NBU



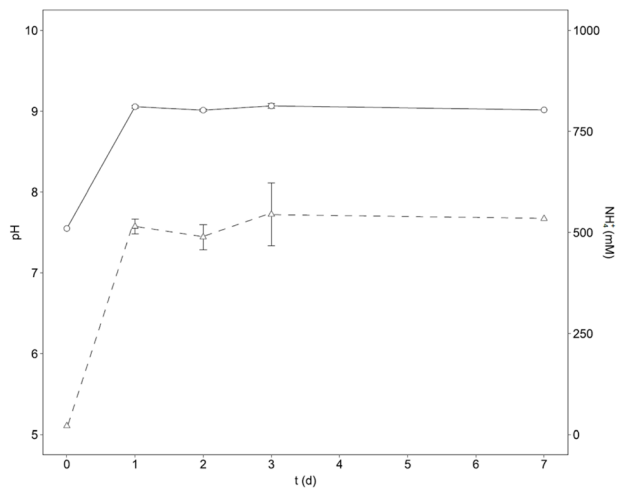


Fig. 6 Evolution of soil pH (left y-axis, circle) and  $\text{NH}_4^+$  (right y-axis, triangle) over time following bioaugmentation of *S. pasteurii* to induce urea hydrolysis in polluted soil from a gas plant (COV-14). Markers and error bars indicate the average and standard deviation of three replicate samples.

has been used in both bioaugmentation<sup>4,5,7</sup> and biostimulation,<sup>12</sup> and LBU in bioaugmentation<sup>6</sup> experiments to stimulate multiple ureolytic bacteria. Other researchers have used tryptic soy broth and acetate,<sup>77</sup> acetate minimal agar<sup>3</sup> and DSMZ nutrient broth.<sup>9</sup> This inconsistency in our experimental design could have resulted in changes in COV14 biostimulation experiments however the different media used in the literature does not support it. The environmental conditions of bioaugmentation and biostimulation experiments in this study were equal, and similar to other studies (e.g.,<sup>10,77</sup>). Our results support that the total amount of viable cell numbers/amount of available urease enzyme might be critical to overcome urease inhibition (Fig. 5), which is further supported by other bioaugmentation studies which have used high cell inoculation concentrations ( $\text{OD}_{600} = 1$  and  $10^{7-9}$  cells  $\text{mL}^{-1}$ ) in heavily polluted soils.<sup>8-10,77</sup> We encourage future studies to focus on treatment parameter optimisation (e.g., minimum cell concentration, reaction time, media/cell injection flow rate cycles) associated with bioaugmentation approaches, larger scale mesocosm experiments (e.g., soil columns), and treatments including calcium to induce calcium carbonate precipitation.

## Conclusions

Persistent pollutants such as polycyclic aromatic hydrocarbons often co-exist with heavy metals in polluted soil environments where they can reduce or inhibit altogether ureolysis critical for the effectiveness of microbial and enzyme induced calcite precipitation for heavy metal bioremediation. Overall, this study concludes that where hydrocarbons suppress soil ureolysis by autochthonous bacteria, bioaugmentation approaches with *S. pasteurii* and soybean *Glycine Max* urease enzyme could induce favourable environmental conditions for the precipitation of calcium carbonate minerals through ureolysis. The insignificant negative effect of hydrocarbons on cell and

enzyme urease activity at sufficient enzyme/cell concentration indicate hydrocarbon mechanism of ureolysis inhibition was competitive and sufficient cell/enzyme inoculation (e.g.,  $\text{OD}_{600} = 1$ ; 100 g bean  $\text{L}^{-1}$ ) would be required to overcome it. Cell growth kinetics and membrane stability were unaffected even at the highest contaminant and low initial cell concentration ( $\text{OD}_{600} = 0.01$ ), indicating *S. pasteurii* ability to thrive in hydrocarbon polluted environments and the negative effects mainly occurred at enzymatic level. These results further suggested bacteria was potentially able to utilise additional carbon sources, and we speculate this could include PAH. The results of this study widen the scope of MICP bioremediation applications to environments co-polluted by heavy metals and hydrocarbons, relevant in both anthropogenic and ecological settings.

## Author contributions

CCC (conceptualisation, data curation, formal analysis, investigation, methodology, resources, supervision, writing – original draft), PJS (methodology, writing – review & editing), AO (investigation, data curation, formal analysis, methodology, writing – original draft), FC (methodology, writing – review & editing), VBG (investigation, data curation, writing – original draft), WTS (writing – review & editing), CJS (writing – review & editing), AMB (conceptualization, funding acquisition, supervision, writing – review & editing), JM (conceptualization, funding acquisition, supervision, writing – review & editing), CU (conceptualization, funding acquisition, project administration, supervision, writing – review & editing), CGL (conceptualization, funding acquisition, methodology, project administration, supervision, writing – review & editing).

## Conflicts of interest

There are no conflicts to declare.

## Data availability

The data is available at: <https://doi.org/10.5525/gla.researchdata.2075>.

Supplementary information is available. See DOI: <https://doi.org/10.1039/d5em00531k>.

## Acknowledgements

This work has been conducted as part of the GALLANT project and is funded by the Natural Environment Research Council as part of the Changing the Environment Programme [grant number NE/W005042/1]. Special thanks are given to the funding body UKRI Natural Environment Research Council, to A. Hunter, E. Palmer, Dr C. Brolly, K. Roberts of the University of Glasgow for their technical support, to Dr V. Olive and Dr G. MacKinnon of the Scottish Universities Environmental Research Centre (SUERC) for the expert advice and analysis of samples, to E. Murray of the GALLANT research project for the administrative support, and to Dr G. El Mountassir of



Strathclyde University and J. Fraser of Hugh King Tillicoultry Quarries for sourcing materials.

## Notes and references

- 1 FAO and UNEP, *Global Assessment of Soil Pollution: Report*, Rome, 2021, DOI: [10.4060/cb4894en](https://doi.org/10.4060/cb4894en).
- 2 L. Chai, S. Huang, Z. Yang, B. Peng, Y. Huang and Y. Chen, Cr (VI) remediation by indigenous bacteria in soils contaminated by chromium-containing slag, *J. Hazard Mater.*, 2009, **167**(1–3), 516–522, DOI: [10.1016/j.jhazmat.2009.01.030](https://doi.org/10.1016/j.jhazmat.2009.01.030).
- 3 V. Achal, X. Pan, D. J. Lee, D. Kumari and D. Zhang, Remediation of Cr (VI) from chromium slag by biocementation, *Chemosphere*, 2013, **93**(7), 1352–1358, DOI: [10.1016/j.chemosphere.2013.08.008](https://doi.org/10.1016/j.chemosphere.2013.08.008).
- 4 D. Kumari, M. Li, X. Pan and Q. Xin-Yi, Effect of bacterial treatment on Cr (VI) remediation from soil and subsequent plantation of *Pisum sativum*, *Ecol. Eng.*, 2014, **73**, 404–408, DOI: [10.1016/j.ecoleng.2014.09.093](https://doi.org/10.1016/j.ecoleng.2014.09.093).
- 5 V. Achal, X. Pan, D. Zhang and Q. Fu, Bioremediation of Pb-contaminated soil based on microbially induced calcite precipitation, *J. Microbiol. Biotechnol.*, 2012, **22**(2), 244–247, DOI: [10.4014/jmb.1108.08033](https://doi.org/10.4014/jmb.1108.08033).
- 6 M. Govarthan, K. J. Lee, M. Cho, J. S. Kim, S. Kamala-Kannan and B. T. Oh, Significance of autochthonous *Bacillus* sp. KK1 on biomineralization of lead in mine tailings, *Chemosphere*, 2013, **90**(8), 2267–2272, DOI: [10.1016/j.chemosphere.2012.10.038](https://doi.org/10.1016/j.chemosphere.2012.10.038).
- 7 V. Achal, X. Pan and D. Zhang, Bioremediation of strontium (Sr) contaminated aquifer quartz sand based on carbonate precipitation induced by Sr resistant *Halomonas* sp, *Chemosphere*, 2012, **89**(6), 764–768, DOI: [10.1016/j.chemosphere.2012.06.064](https://doi.org/10.1016/j.chemosphere.2012.06.064).
- 8 J. Yang, X. Pan, C. Zhao, S. Mou, V. Achal, F. A. Al-Misned, M. G. Mortuza and G. M. Gadd, Bioimmobilization of heavy metals in acidic copper mine tailings soil, *Geomicrobiol. J.*, 2016, **33**(3–4), 261–266, DOI: [10.1080/01490451.2015.1068889](https://doi.org/10.1080/01490451.2015.1068889).
- 9 P. Liu, Y. Zhang, Q. Tang and S. Shi, Bioremediation of metal-contaminated soils by microbially-induced carbonate precipitation and its effects on ecotoxicity and long-term stability, *Biochem. Eng. J.*, 2021, **166**, 107856, DOI: [10.1016/j.bej.2020.107856](https://doi.org/10.1016/j.bej.2020.107856).
- 10 V. Achal, X. Pan, Q. Fu and D. Zhang, Biomineralization based remediation of As (III) contaminated soil by *Sporosarcina ginsengisoli*, *J. Hazard Mater.*, 2012, **201**, 178–184, DOI: [10.1016/j.jhazmat.2011.11.067](https://doi.org/10.1016/j.jhazmat.2011.11.067).
- 11 X. Zhu, W. Li, L. Zhan, M. Huang, Q. Zhang and V. Achal, The large-scale process of microbial carbonate precipitation for nickel remediation from an industrial soil, *Environ. Pollut.*, 2016, **219**, 149–155, DOI: [10.1016/j.envpol.2016.10.047](https://doi.org/10.1016/j.envpol.2016.10.047).
- 12 X. Chen and V. Achal, Biostimulation of carbonate precipitation process in soil for copper immobilization, *J. Hazard Mater.*, 2019, **368**, 705–713, DOI: [10.1016/j.jhazmat.2019.01.108](https://doi.org/10.1016/j.jhazmat.2019.01.108).
- 13 Y. F. Li, S. Hao, W. L. Ma, P. F. Yang, W. L. Li, Z. F. Zhang, L. Y. Liu and R. W. Macdonald, Persistent organic pollutants in global surface soils: distributions and fractionations, *Environ. Sci. Ecotechnology*, 2024, **18**, 100311, DOI: [10.1016/j.esc.2023.100311](https://doi.org/10.1016/j.esc.2023.100311).
- 14 E. Heywood, J. Wright, C. L. Wienburg, H. I. Black, S. M. Long, D. Osborn and D. J. Spurgeon, Factors influencing the national distribution of polycyclic aromatic hydrocarbons and polychlorinated biphenyls in British soils, *Environ. Sci. Technol.*, 2006, **40**(24), 7629–7635, DOI: [10.1021/es061296x](https://doi.org/10.1021/es061296x).
- 15 S. Ye, G. Zeng, H. Wu, C. Zhang, J. Liang, J. Dai, Z. Liu, W. Xiong, J. Wan, P. Xu and M. Cheng, Co-occurrence and interactions of pollutants, and their impacts on soil remediation—a review, *Crit. Rev. Environ. Sci. Technol.*, 2017, **47**(16), 1528–1553, DOI: [10.1080/10643389.2017.1386951](https://doi.org/10.1080/10643389.2017.1386951).
- 16 J. T. Dejong, K. Soga, E. Kavazanjian, S. Burns, L. A. Van Paassen, A. Al Qabany, A. Aydilek, S. S. Bang, M. Burbank, L. F. Caslake and C. Y. Chen, Biogeochemical processes and geotechnical applications: progress, opportunities and challenges, in: *Bio-and Chemo-Mechanical Processes in Geotechnical Engineering: Géotechnique Symposium in Print 2013 2014*, Ice Publishing, pp. , pp. 143–157, DOI: [10.1680/bcmpge.60531.014](https://doi.org/10.1680/bcmpge.60531.014).
- 17 M. B. Burbank, T. J. Weaver, B. C. Williams and R. L. Crawford, Urease activity of ureolytic bacteria isolated from six soils in which calcite was precipitated by indigenous bacteria, *Geomicrobiol. J.*, 2012, **29**(4), 389–395, DOI: [10.1080/01490451.2011.575913](https://doi.org/10.1080/01490451.2011.575913).
- 18 J. K. Mitchell and J. C. Santamarina, Biological considerations in geotechnical engineering, *J. Geotech. Geoenviron. Eng.*, 2005, **131**(10), 1222–1233, DOI: [10.1061/\(ASCE\)1090-0241\(2005\)131:10\(1222\)](https://doi.org/10.1061/(ASCE)1090-0241(2005)131:10(1222)).
- 19 B. M. Mortensen, M. J. Haber, J. T. DeJong, L. F. Caslake and D. C. Nelson, Effects of environmental factors on microbial induced calcium carbonate precipitation, *J. Appl. Microbiol.*, 2011, **111**(2), 338–349, DOI: [10.1111/j.1365-2672.2011.05065.x](https://doi.org/10.1111/j.1365-2672.2011.05065.x).
- 20 V. Stabnikov, C. Jian, V. Ivanov and Y. Li, Halotolerant, alkaliphilic urease-producing bacteria from different climate zones and their application for biocementation of sand, *World J. Microbiol. Biotechnol.*, 2013, **29**, 1453–1460, DOI: [10.1007/s11274-013-1309-1](https://doi.org/10.1007/s11274-013-1309-1).
- 21 L. Cheng, M. A. Shahin, R. Cord-Ruwisch, M. Addis, T. Hartanto and C. Elms, Soil stabilisation by microbial-induced calcite precipitation (MICP): investigation into some physical and environmental aspects, in: *7th international congress on environmental geotechnics*, Engineers Australia Melbourne, Australia, 2014, vol. 64, 12, pp. 1105–1112.
- 22 D. Gat, Z. Ronen and M. Tsesarsky, Long-term sustainability of microbial-induced CaCO<sub>3</sub> precipitation in aqueous media, *Chemosphere*, 2017, **184**, 524–531, DOI: [10.1016/j.chemosphere.2017.06.015](https://doi.org/10.1016/j.chemosphere.2017.06.015).
- 23 R. Margesin, G. Walder and F. Schinner, The impact of hydrocarbon remediation (diesel oil and polycyclic



- aromatic hydrocarbons) on enzyme activities and microbial properties of soil, *Acta Biotechnol.*, 2000, **20**(3-4), 313–333, DOI: [10.1002/abio.370200312](https://doi.org/10.1002/abio.370200312).
- 24 R. Margesin, A. Zimmerbauer and F. Schinner, Monitoring of bioremediation by soil biological activities, *Chemosphere*, 2000, **40**(4), 339–346, DOI: [10.1016/S0045-6535\(99\)00218-0](https://doi.org/10.1016/S0045-6535(99)00218-0).
- 25 C. Trasar-Cepeda, M. C. Leiros, S. Seoane and F. Gil-Sotres, Limitations of soil enzymes as indicators of soil pollution, *Soil Biol. Biochem.*, 2000, **32**(13), 1867–1875, DOI: [10.1016/S0038-0717\(00\)00160-7](https://doi.org/10.1016/S0038-0717(00)00160-7).
- 26 E. Dindar, F. O. Şağban and H. S. Başkaya, Variations of soil enzyme activities in petroleum-hydrocarbon contaminated soil, *Int. Biodeterior. Biodegrad.*, 2015, **105**, 268–275, DOI: [10.1016/j.ibiod.2015.09.011](https://doi.org/10.1016/j.ibiod.2015.09.011).
- 27 S. Baran, J. E. Bielińska and P. Oleszczuk, Enzymatic activity in an airfield soil polluted with polycyclic aromatic hydrocarbons, *Geoderma*, 2004, **118**(3–4), 221–232, DOI: [10.1016/S0016-7061\(03\)00205-2](https://doi.org/10.1016/S0016-7061(03)00205-2).
- 28 H. Guo, J. Yao, M. Cai, Y. Qian, Y. Guo, H. H. Richnow, R. E. Blake, S. Doni and B. Ceccanti, Effects of petroleum contamination on soil microbial numbers, metabolic activity and urease activity, *Chemosphere*, 2012, **87**(11), 1273–1280, DOI: [10.1016/j.chemosphere.2012.01.034](https://doi.org/10.1016/j.chemosphere.2012.01.034).
- 29 V. Andreoni, L. Cavalca, M. A. Rao, G. Nocerino, S. Bernasconi, E. Dell'Amico, M. Colombo and L. Gianfreda, Bacterial communities and enzyme activities of PAHs polluted soils, *Chemosphere*, 2004, **57**(5), 401–412, DOI: [10.1016/j.chemosphere.2004.06.013](https://doi.org/10.1016/j.chemosphere.2004.06.013).
- 30 G. Shen, Y. Lu and J. Hong, Combined effect of heavy metals and polycyclic aromatic hydrocarbons on urease activity in soil, *Ecotoxicol. Environ. Saf.*, 2006, **63**(3), 474–480, DOI: [10.1016/j.ecoenv.2005.01.009](https://doi.org/10.1016/j.ecoenv.2005.01.009).
- 31 J. Wyzkowska and M. Wyzkowski, Activity of soil dehydrogenases, urease, and acid and alkaline phosphatases in soil polluted with petroleum, *J. Toxicol. Environ. Health, Part A*, 2010, **73**(17–18), 1202–1210, DOI: [10.1080/15287394.2010.492004](https://doi.org/10.1080/15287394.2010.492004).
- 32 B. Wu, T. Lan, D. Lu and Z. Liu, Ecological and enzymatic responses to petroleum contamination, *Environ. Sci.: Processes Impacts*, 2014, **16**(6), 1501–1509, DOI: [10.1039/C3EM00731F](https://doi.org/10.1039/C3EM00731F).
- 33 H. Feyzi, M. Chorom and G. Bagheri, Urease activity and microbial biomass of carbon in hydrocarbon contaminated soils. A case study of cheshmeh-khosh oil field, Iran, *Ecotoxicol. Environ. Saf.*, 2020, **199**, 110664, DOI: [10.1016/j.ecoenv.2020.110664](https://doi.org/10.1016/j.ecoenv.2020.110664).
- 34 M. N. Moore, Cellular responses to pollutants, *Mar. Pollut. Bull.*, 1985, **16**(4), 134–139, DOI: [10.1016/0025-326X\(85\)90003-7](https://doi.org/10.1016/0025-326X(85)90003-7).
- 35 M. N. Moore and S. V. Farrar, Effects of polynuclear aromatic hydrocarbons on lysosomal membranes in molluscs, *Mar. Environ. Res.*, 1985, **17**(2–4), 222–225, DOI: [10.1016/0141-1136\(85\)90091-1](https://doi.org/10.1016/0141-1136(85)90091-1).
- 36 L. E. Sverdrup, T. Nielsen and P. H. Krogh, Soil ecotoxicity of polycyclic aromatic hydrocarbons in relation to soil sorption, lipophilicity, and water solubility, *Environ. Sci. Technol.*, 2002, **36**(11), 2429–2435, DOI: [10.1021/es010180s](https://doi.org/10.1021/es010180s).
- 37 Y. Liu, Q. Dai, X. Jin, X. Dong, J. Peng, M. Wu, N. Liang, B. Pan and B. Xing, Negative impacts of biochars on urease activity: high pH, heavy metals, polycyclic aromatic hydrocarbons, or free radicals?, *Environ. Sci. Technol.*, 2018, **52**(21), 12740–12747, DOI: [10.1021/acs.est.8b00672](https://doi.org/10.1021/acs.est.8b00672).
- 38 B. Krajewska and I. Ureases, Functional, catalytic and kinetic properties: A review, *J. Mol. Catal. B:Enzym.*, 2009, **59**(1–3), 9–21, DOI: [10.1016/j.molcatb.2009.01.003](https://doi.org/10.1016/j.molcatb.2009.01.003).
- 39 C. Gauchotte-Lindsay, T. J. Aspray, M. Knapp and U. Z. Ijaz, Systems biology approach to elucidation of contaminant biodegradation in complex samples—integration of high-resolution analytical and molecular tools, *Faraday Discuss.*, 2019, **218**, 481–504, DOI: [10.1039/C9FD00020H](https://doi.org/10.1039/C9FD00020H).
- 40 C. Comadran-Casas, C. Unluer, A. M. Bass, J. Macdonald, E. K. Najafi, L. Spruzeniece and C. Gauchotte-Lindsay, Bioremediation of multiple heavy metals through biostimulation of microbial-induced calcite precipitation at varying calcium-to-urea concentrations, *J. Hazard. Mater.*, 2025, **491**, 137691, DOI: [10.1016/j.jhazmat.2025.137691](https://doi.org/10.1016/j.jhazmat.2025.137691).
- 41 L. S. Lee, P. S. Rao and I. Okuda, Equilibrium partitioning of polycyclic aromatic hydrocarbons from coal tar into water, *Environ. Sci. Technol.*, 1992, **26**(11), 2110–2115.
- 42 J. L. Collier, B. Brahamsha and B. Palenik, The marine cyanobacterium *Synechococcus* sp. WH7805 requires urease (urea amiohydrolase, EC 3.5. 1.5) to utilize urea as a nitrogen source: molecular-genetic and biochemical analysis of the enzyme, *Microbiology*, 1999, **145**(2), 447–459, DOI: [10.1099/13500872-145-2-447](https://doi.org/10.1099/13500872-145-2-447).
- 43 T. L. Gresham, P. P. Sheridan, M. E. Watwood, Y. Fujita and F. S. Colwell, Design and validation of ure C-based primers for groundwater detection of urea-hydrolyzing bacteria, *Geomicrobiol. J.*, 2007, **24**(3–4), 353–364, DOI: [10.1080/01490450701459283](https://doi.org/10.1080/01490450701459283).
- 44 Z. Wang, K. Feng, Z. Wei, Y. Wu, K. Isobe, K. Senoo, X. Peng, D. Wang, Q. He, X. Du and S. Li, Evaluation and redesign of the primers for detecting nitrogen cycling genes in environments, *Methods Ecol. Evol.*, 2022, **13**(9), 1976–1989, DOI: [10.1111/2041-210X.13946](https://doi.org/10.1111/2041-210X.13946).
- 45 X. Li, J. Manuel, S. Slavens, D. W. Crunkleton and T. W. Johannes, Interactive effects of light quality and culturing temperature on algal cell size, biomass doubling time, protein content, and carbohydrate content, *Appl. Microbiol. Biotechnol.*, 2021, **105**, 587–597, DOI: [10.1007/s00253-020-11068-y](https://doi.org/10.1007/s00253-020-11068-y).
- 46 M. D. Rolfe, C. J. Rice, S. Lucchini, C. Pin, A. Thompson, A. D. Cameron, M. Alston, M. F. Stringer, R. P. Betts, J. Baranyi and M. W. Peck, Lag phase is a distinct growth phase that prepares bacteria for exponential growth and involves transient metal accumulation, *J. Bacteriol.*, 2012, **194**(3), 686–701, DOI: [10.1128/jb.06112-11](https://doi.org/10.1128/jb.06112-11).
- 47 J. A. Myers, B. S. Curtis and W. R. Curtis, Improving accuracy of cell and chromophore concentration measurements using optical density, *BMC Biophys.*, 2013, **6**, 1–6, DOI: [10.1186/2046-1682-6-4](https://doi.org/10.1186/2046-1682-6-4).



- 48 T. Falcioni, S. Papa and J. M. Gasol, Evaluating the flow-cytometric nucleic acid double-staining protocol in realistic situations of planktonic bacterial death, *Appl. Environ. Microbiol.*, 2008, **74**(6), 1767–1779, DOI: [10.1128/AEM.01668-07](https://doi.org/10.1128/AEM.01668-07).
- 49 J. L. Nielsen, C. Kragelund and P. H. Nielsen, Combination of fluorescence *in situ* hybridization with staining techniques for cell viability and accumulation of PHA and polyP in microorganisms in complex microbial systems, in: *Bioremediation: Methods and Protocols*, Humana Press, Totowa, NJ, 2009, 25 pp. 103–116.
- 50 M. Vignola, D. Werner, F. Hammes, L. C. King and R. J. Davenport, Flow-cytometric quantification of microbial cells on sand from water biofilters, *Water Res.*, 2018, **143**, 66–76, DOI: [10.1016/j.watres.2018.05.053](https://doi.org/10.1016/j.watres.2018.05.053).
- 51 B. G. Hall, H. Acar, A. Nandipati and M. Barlow, Growth rates made easy, *Mol. Biol. Evol.*, 2014, **31**(1), 232–238, DOI: [10.1093/molbev/mst187](https://doi.org/10.1093/molbev/mst187).
- 52 J. M. Minto, Q. Tan, R. J. Lunn, G. El Mountassir, H. Guo and X. Cheng, 'Microbial mortar'-restoration of degraded marble structures with microbially induced carbonate precipitation, *Constr. Build. Mater.*, 2018, **180**, 44–54, DOI: [10.1016/j.conbuildmat.2018.05.200](https://doi.org/10.1016/j.conbuildmat.2018.05.200).
- 53 Y. Weng, H. Lai, J. Zheng, M. Cui, Y. Chen, Z. Xu, W. Jiang, J. Zhang and Y. Song, Effect of acid type on biomineralization of soil using crude soybean urease solution, *J. Rock Mech. Geotech. Eng.*, 2024, **16**(12), 5135–5146, DOI: [10.1016/j.jrmge.2024.09.017](https://doi.org/10.1016/j.jrmge.2024.09.017).
- 54 V. S. Whiffin, Microbial CaCO<sub>3</sub> precipitation for the production of biocement [Murdoch University], 2004, <https://researchportal.murdoch.edu.au/esploro/outputs/doctoral/Microbial-CaCO3-precipitation-for-the-production/991005540291407891#file-0>.
- 55 A. P. Tessier, P. G. Campbell and M. J. Bisson, Sequential extraction procedure for the speciation of particulate trace metals, *Anal. Chem.*, 1979, **51**(7), 844–851.
- 56 M. A. Tabatabai, Effects of trace elements on urease activity in soils, *Soil Biol. Biochem.*, 1977, **9**(1), 9–13, DOI: [10.1016/0038-0717\(77\)90054-2](https://doi.org/10.1016/0038-0717(77)90054-2).
- 57 B. Krajewska, Urease immobilized on chitosan membrane. Inactivation by heavy metal ions, *J. Chem. Technol. Biotechnol.*, 1991, **52**(2), 157–162, DOI: [10.1002/jctb.280520203](https://doi.org/10.1002/jctb.280520203).
- 58 W. Zaborska, B. Krajewska and Z. Olech, Heavy metal ions inhibition of jack bean urease: potential for rapid contaminant probing, *J. Enzyme Inhib. Med. Chem.*, 2004, **19**(1), 65–69, DOI: [10.1080/14756360310001650237](https://doi.org/10.1080/14756360310001650237).
- 59 L. Fang, Q. Niu, L. Cheng, J. Jiang, Y. Y. Yu, J. Chu, V. Achal and T. You, Ca-mediated alleviation of Cd<sup>2+</sup> induced toxicity and improved Cd<sup>2+</sup> biomineralization by *Sporosarcina pasteurii*, *Sci. Total Environ.*, 2021, **787**, 147627, DOI: [10.1016/j.scitotenv.2021.147627](https://doi.org/10.1016/j.scitotenv.2021.147627).
- 60 A. J. Mugwar and M. J. Harbottle, Toxicity effects on metal sequestration by microbially-induced carbonate precipitation, *J. Hazard. Mater.*, 2016, **314**, 237–248, DOI: [10.1016/j.jhazmat.2016.04.039](https://doi.org/10.1016/j.jhazmat.2016.04.039).
- 61 N. J. Jiang, R. Liu, Y. J. Du and Y. Z. Bi, Microbial induced carbonate precipitation for immobilizing Pb contaminants: Toxic effects on bacterial activity and immobilization efficiency, *Sci. Total Environ.*, 2019, **672**, 722–731, DOI: [10.1016/j.scitotenv.2019.03.294](https://doi.org/10.1016/j.scitotenv.2019.03.294).
- 62 C. H. Kang, S. J. Oh, Y. Shin, S. H. Han, I. H. Nam and J. S. So, Bioremediation of lead by ureolytic bacteria isolated from soil at abandoned metal mines in South Korea, *Ecol. Eng.*, 2015, **74**, 402–407, DOI: [10.1016/j.ecoleng.2014.10.009](https://doi.org/10.1016/j.ecoleng.2014.10.009).
- 63 S. Qiao, G. Zeng, X. Wang, C. Dai, M. Sheng, Q. Chen, F. Xu and H. Xu, Multiple heavy metals immobilization based on microbially induced carbonate precipitation by ureolytic bacteria and the precipitation patterns exploration, *Chemosphere*, 2021, **274**, 129661, DOI: [10.1016/j.chemosphere.2021.129661](https://doi.org/10.1016/j.chemosphere.2021.129661).
- 64 J. A. Sikkema, J. A. de Bont and B. Poolman, Mechanisms of membrane toxicity of hydrocarbons, *Microbiol. Rev.*, 1995, **59**(2), 201–222, DOI: [10.1128/mr.59.2.201-222.1995](https://doi.org/10.1128/mr.59.2.201-222.1995).
- 65 C. E. Cerniglia, Microbial metabolism of polycyclic aromatic hydrocarbons, *Adv. Appl. Microbiol.*, 1984, **30**, 31–71, DOI: [10.1016/S0065-2164\(08\)70052-2](https://doi.org/10.1016/S0065-2164(08)70052-2).
- 66 R. A. Kanaly and S. Harayama, Biodegradation of high-molecular-weight polycyclic aromatic hydrocarbons by bacteria, *J. Bacteriol.*, 2000, **182**(8), 2059–2067, DOI: [10.1128/jb.182.8.2059-2067.2000](https://doi.org/10.1128/jb.182.8.2059-2067.2000).
- 67 S. Boonchan, M. L. Britz and G. A. Stanley, Degradation and mineralization of high-molecular-weight polycyclic aromatic hydrocarbons by defined fungal-bacterial cocultures, *Appl. Environ. Microbiol.*, 2000, **66**(3), 1007–1019, DOI: [10.1128/AEM.66.3.1007-1019.2000](https://doi.org/10.1128/AEM.66.3.1007-1019.2000).
- 68 N. Mangwani, S. Kumari and S. Das, Involvement of quorum sensing genes in biofilm development and degradation of polycyclic aromatic hydrocarbons by a marine bacterium *Pseudomonas aeruginosa* N6P6, *Appl. Microbiol. Biotechnol.*, 2015, **99**, 10283–10297, DOI: [10.1007/s00253-015-6868-7](https://doi.org/10.1007/s00253-015-6868-7).
- 69 A. Lipińska, J. Kucharski and J. Wyzkowska, Urease activity in soil contaminated with polycyclic aromatic hydrocarbons, *Pol. J. Environ. Stud.*, 2013, **22**(5), 1393–1400.
- 70 E. M. Murphy, J. M. Zachara and S. C. Smith, Influence of mineral-bound humic substances on the sorption of hydrophobic organic compounds, *Environ. Sci. Technol.*, 1990, **24**(10), 1507–1516.
- 71 J. J. Pignatello and B. Xing, Mechanisms of slow sorption of organic chemicals to natural particles, *Environ. Sci. Technol.*, 1995, **30**(1), 1–11, DOI: [10.1021/es940683g](https://doi.org/10.1021/es940683g).
- 72 L. Liu, Y. Gao, W. Geng, J. Song, Y. Zhou and C. Li, Comparison of jack bean and soybean crude ureases on surface stabilization of desert sand *via* enzyme-induced carbonate precipitation, *Geoderma*, 2023, **435**, 116504, DOI: [10.1016/j.geoderma.2023.116504](https://doi.org/10.1016/j.geoderma.2023.116504).
- 73 E. G. Lauchnor, D. M. Topp, A. E. Parker and R. Gerlach, Whole cell kinetics of ureolysis by *Sporosarcina pasteurii*, *J. Appl. Microbiol.*, 2015, **118**(6), 1321–1332, DOI: [10.1111/jam.12804](https://doi.org/10.1111/jam.12804).
- 74 N. M. Pettit, A. R. Smith, R. B. Freedman and R. G. Burns, Soil urease: activity, stability and kinetic properties, *Soil*



- Biol. Biochem.*, 1976, **8**(6), 479–484, DOI: [10.1016/0038-0717\(76\)90089-4](https://doi.org/10.1016/0038-0717(76)90089-4).
- 75 A. Ukalska-Jaruga and B. Smreczak, The impact of organic matter on polycyclic aromatic hydrocarbon (PAH) availability and persistence in soils, *Molecules*, 2020, **25**(11), 2470, DOI: [10.3390/molecules25112470](https://doi.org/10.3390/molecules25112470).
- 76 S. Svane, J. J. Sigurdarson, F. Finkenwirth, T. Eitinger and H. Karring, Inhibition of urease activity by different compounds provides insight into the modulation and association of bacterial nickel import and ureolysis, *Sci. Rep.*, 2020, **10**(1), 8503, DOI: [10.1038/s41598-020-65107-9](https://doi.org/10.1038/s41598-020-65107-9).
- 77 H. Chung, S. H. Kim and K. Nam, Inhibition of urea hydrolysis by free Cu concentration of soil solution in microbially induced calcium carbonate precipitation, *Sci. Total Environ.*, 2020, **740**, 140194, DOI: [10.1016/j.scitotenv.2020.140194](https://doi.org/10.1016/j.scitotenv.2020.140194).

